RSC Advances

ROYAL SOCIETY OF CHEMISTRY

www.rsc.org/advances

Molecular dynamics and dissipative particle dynamics simulations of miscibility and mechanical properties of GAP/DIANP blending systems

Junqing Yang[1], Xueli Zhang[1], Pin Gao[2], Xuedong Gong[1*], Guixiang Wang[1*]

1.Department of Chemistry, Nanjing University of Science and Technology, Nanjing 210094, China

2.National Civil Blasting Equipment Quality Supervision and Testing Center, Nanjing 210094, China

Abstract

Molecular dynamics (MD) and dissipative particle dynamics (DPD) simulations were performed to investigate the compatibility and mechanical properties of GAP (glycidyl azido polymer, an azido binder) and DIANP (1, 5-diazido-3-nitrazapentane, an azido plasticizer). To determine the appropriate simulated chain length (n) of GAP, the solubility parameter (δ) was examined under n=5, 10, 20, 30, and 40. The obtained δ decreases with the increasing n and when n reaches to 20, δ changes little and gives good agreements with the experimental data. Considering the computational costs, the chain length of GAP was selected to be 20. Then a series of blending systems of GAP (n=20) and DIANP with mass ratios of 78.4/21.6 (I), 57.7/42.3 (II), and 37.7/62.3 (III) were constructed and studied. Results of solubility parameters, Flory-Huggins interaction parameters, blend binding energy distributions and mesoscopic morphologies all show that GAP and DIANP have a good miscibility with each other. Compared with the mechanical properties of the pure GAP, it is found that addition of DIANP can enhance the plastic property of GAP and the blend II has the best tenacity and ductility.

Keywords MD, DPD, GAP, DIANP, mechanical property, miscibility

1 Introduction

Composite solid propellants are a major resource for space vehicles and missiles. Generally, their formulations include a binder, a plasticizer, a high-energetic filler, bonding and curing agents, a burning rate modifier, and so on [1]. Glycidyl azido polymer (GAP) as an energetic binder has received considerable interests. The major advantages of GAP over the

* Corresponding authors. E-mail: gongxd325@mail.njust.edu.cn; wanggx1028@163.com
Tel: +86-25-84315947-803

commonly used energetic binders such as hydroxyl-terminated polybutadiene (HTPB) include higher energy output, higher density, and better compatibility with high energetic oxidizers such as ammonium dinitramide (ADN) and hydrazinium nitroformate (HNF) [2], which results in higher specific impulses for the propellant formulations with GAP as energetic binder. However, GAP suffers from poor mechanical properties under low temperatures. To overcome this problem, methods such as constructing blends or copolymers have been proposed [3-4] and many researchers have devoted to finding better plasticizers to enhance the mechanical properties of GAP, especially under the low temperature. Compared with nitrate esters plasticizers, azido plasticizers have better compatibility with azido binders [5]. Despite of the better compatibility, the specific miscibility of azido plasticizers with azido binders remains elusive.

Molecular dynamic (MD) simulation is the most widely used method to simulate the dynamics of atomistic systems and has been widely used to predict the miscibility and the mechanical properties of blending systems. However, the MD method is limited to simulate the dynamics of a few thousands of molecules over a few nanoseconds with current computers. Dissipative particle dynamics (DPD) is a mesoscale simulation method. It can provide a dynamics algorithm with hydrodynamics for studying coarse-grained systems over long length and time scales. Moreover, DPD simulation is capable of providing valuable mesoscopic morphologies of the actual polymer systems and revealing the microscopic pictures of underlying mechanisms [6-8]. Therefore, in this work, MD and DPD simulations were carried out together to study the binary blends of GAP and DIANP (1, 5-diazido-3-nitrazapentane). DIANP is a kind of azido plasticizer with smaller impact and friction sensitivities than the conventional plasticizer NG (nitroglycerin) and better compatibility with NC (nitrocellulose). It has attracted many experimental and theoretical attentions [9-11]. We mainly investigate (I) the compatibility of GAP and DIANP and (II) whether DIANP has positive effects on the mechanical properties of GAP.

This study gives the first insight into the mechanical properties and provides a first mesoscopic understanding of the miscibility of various GAP/DIANP blending systems. We

believe it is helpful for better understanding the azido plasticizer DIANP and the plasticizing systems of GAP.

2. Computational model and details

2.1 Molecular dynamics simulation

Determination of the right chain length is the first step for the MD simulation of polymer. Since short chains might lead to end effects and cannot represent the real systems accurately, while long chains may lead to difficulties for computer simulations [12]. To determine the appropriate chain lengths (*n*), GAP chains with *n*=5, 10, 20, 30, and 40 were constructed using the Visualizer module of Materials Studio (MS) [13]. These chains were first optimized using the "Smart Minimizer" algorithm until the root-mean-square of the potential energy gradient being less than 0.001 kcal.mol^{-1}.Å^{-1}, and then piled into the amorphous unit with the specified density using the Amorphous cell module and 3D periodic boundary conditions. Table 1 lists the initial densities, the number of units, chains and atoms, and the weights of DIANP and GAP with different *n* (GAP1, GAP2, GAP3, GAP4, and GAP5).

Table 1 Pure DIANP and GAP in MD simulations

	Initial density (g.cm^{-3})	Number of units in a chain	Number of chains / molecules	Number of atoms	Weight of molecule
GAP1	1.30	5	20	1260	10080
GAP2	1.30	10	10	1230	10089
GAP3	1.30	20	5	1216	10000
GAP4	1.30	30	4	1452	11996
GAP5	1.30	40	3	1449	11945
DIANP	1.33		55	1210	11008

For the constructed amorphous models, minimizations were also performed to remove unfavorable interactions and to attain the lowest energy state. Following the energy minimization step, MD simulations were conducted for 200 ps at NVT (constant volume *V* and constant temperature *T*) condition first and then 1000 ps at NpT (constant pressure *p* and constant temperature *T*) condition. There are other ways to perform MD simulations to reach the desired conditions for analyzing statistical quantities. For example, in the works of Wang,

et. al. [14-15], systems were first simulated in the NpT ensemble implementing the Hamiltonian-based thermostat and barostat with the controller frequency of 10^{-4} fs^{-1}. They were equilibrated to the correct density. After the equilibrium density is reached, NVT simulations were conducted for data production. In our NpT simulations, the pressure was set to 0 GPa and the Berendsen barostat which gave the best results in our tests was used. The average pressures from simulations are 0.000002~0.000003 GPa (close to 0 GPa) and the standard deviations are around 0.039 GPa (<0.05 GPa), suggesting that the barostat has been reached. Trajectories were saved every 100 fs and the final 50 ps were used to collect data for statistical analysis of the cohesive energy density and solubility parameter. Solubility parameter (δ) is defined as the square root of the cohesive energy density (*CED*), as shown in Eq. (1).

$$\delta = \sqrt{CED} \tag{1}$$

$$CED=E_{coh}/V \tag{2}$$

$$E_{coh}=\Delta H_v-RT \tag{3}$$

where E_{coh} is the cohesive energy, V is the molar volume, ΔH_v is the molar vaporization heat, and R is the gas constant. Molecular simulation calculation provides an easy way to evaluate the *CED* of polymers and has been used in many studies [16-18]. Comparing the simulated δs with the experimental data, n=20 (GAP3) was determined to be the most appropriate chain length. Fig. 1 depicts the repeat units structure of GAP and molecular structure of DIANP. Fig. 2 shows the initial cell structures of GAP (n=20) and DIANP.

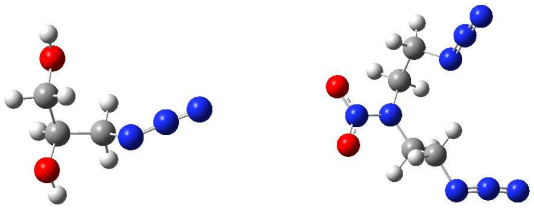

Fig. 1 Repeat unit structure of GAP (left) and molecular structure of DIANP (right)

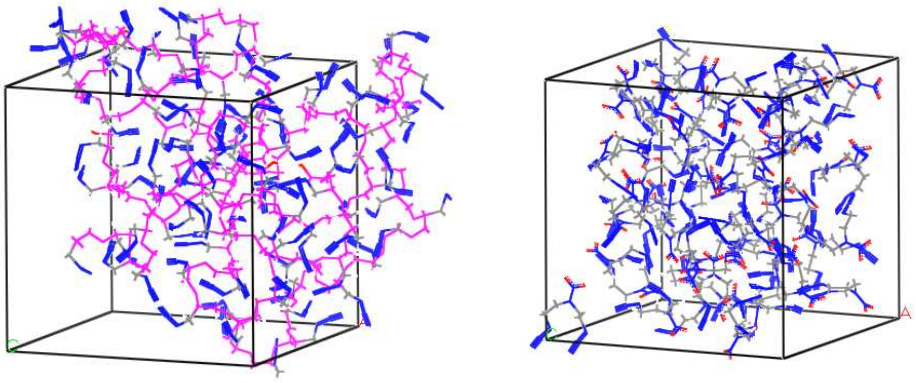

Fig. 2 Initial cell of GAP (n=20, left) and DIANP (right)

Blends of GAP (n=20) and DIANP (GAP/DIANP) with the mass ratio of 78.4/21.6 (I), 57.7/42.3 (II), and 37.7/62.3 (III) were constructed and the relevant parameters (densities, number of chains and atoms, etc.) are shown in Table 2. The blends were then submitted to energy minimizations and MD simulations as were done for pure amorphous models. To search for the most suitable proportion, static elastic properties were analyzed using the final 50 ps of the MD simulations. From the statistical mechanics of elasticity [19], the most general relationship between stress and strain can be stated by the generalized Hooke's law: $\sigma_i = C_{ij}\varepsilon_j$ (i, j = 1-6), where C_{ij} are the elements of the elastic constant matrix, i.e., elastic coefficients. They manifest that there are different elastic effects everywhere in materials. Because of the existence of the strain, the elastic coefficient matrix of a material should satisfy the formula: C_{ij}=C_{ji}, even for an extremely anisotropic body and there are 21 independent elastic coefficients. For an isotropic solid, there are only two independent elastic coefficients (C_{11} and C_{12}). According to the C_{11} and C_{12}, the Lamé coefficients (μ and λ) can be calculated ($C_{11}-C_{12}=2\mu$, $C_{12}=\lambda$). Then, all the elastic modulus, such as tensile (Young's) modulus (E), bulk modulus (K), and shear modulus (G), and Poisson's ratio (γ) can be obtained from the Lamé coefficients (Eq.(4)). The MS program can assume a material as isotropic and give the values of mechanical properties in an output file. The calculation procedure is as follows: For each configuration submitted for static elastic constants analysis, a total of 13 minimizations are performed. The first consists of a conjugate gradients minimization of the undeformed

amorphous system. The target minimum derivative for this is 0.1 kcal/Å. To reduce the time required by the calculation, a maximum of 1000 steps is performed in attempting to satisfy the convergence criterion. Following this initial stage, three tensile and three pure shear deformations of magnitude ±0.0005 are applied to the minimized undeformed system and the system is reminimized following each deformation. The internal stress tensor is then obtained from the analytically calculated virial and used to obtain estimates of the six columns of the elastic stiffness coefficients matrix.

$$E = \frac{\mu(3\lambda+2\mu)}{\lambda+\mu},\ K = \lambda + \frac{2}{3}\mu,\ G = \mu,\quad \gamma = \frac{\lambda}{2(\lambda+\mu)} \tag{4}$$

All MD simulations were performed using the COMPASS force field [20] and run in parallel with eight processors. Temperature controls were treated using Andersen method [21]. The Coulomb and van der Waals long-range nonbonding interactions were handled by using the standard Ewald and Atom-Based summation methods, respectively [22]. Nonbonding interactions, spline width, and buffer width were truncated at 0.95, 0.1 and 0.05 nm, respectively.

Table 2 GAP/DIANP blends with different mass ratios

	Initial density (g.cm^{-3})	Number of chains	Mass ratios	Number of atoms	Weight of molecule
I	1.31	4/11	78.4/21.6	1214	10192
II	1.31	3/22	57.7/42.3	1213	10394
III	1.32	2/33	37.7/62.3	1212	10596

2.2 Dissipative particle dynamics simulation

DPD is a mesoscale method for the simulations of coarse-grained systems over long length and time scales. In DPD, several atoms or repeat units are grouped together and represented by a single bead, thus the algorithm increases simulation scale by several orders of magnitude compared to the atomistic simulation. GAP homopolymer chains are represented by Gaussian chain models (spherical beads connected by harmonic spring), all single and partial bonds in the chains are allowed to rotate during simulations [23]. Each model is composed of several beads, where each bead represents a large number of repeat units of

the molecular chain. Different segments are assumed to have equal volume, which is a necessary assumption to conform with the Flory-Huggins theory and for the dissipative particle dynamics model. The number of beads of a polymer chain in DPD (N_{DPD}) was determined from the following equation:

$$N_{DPD} = \frac{M_p}{M_m C_n} = \frac{n}{C_n} \tag{5}$$

where M_p is the molar mass of the polymer, M_m is the molar mass of the repeat unit, n is the number of repeat units, and C_n is the characteristic ratio of the polymer used to determine how many repeated units should be grouped into one bead. C_n can be evaluated based on the connectivity indices for polymer chain proposed by Bicerano [24] and it was estimated to be 5.299 for GAP. Thus the N_{DPD} of a GAP chain is about 4, that is, five repeat units of GAP makes up one bead and four beads represent a chain of GAP to simulate the coarse-grained model. For DIANP, one molecule represents one bead. Molecular structures and coarse-grained models of GAP and DIANP are depicted in Fig. 3.

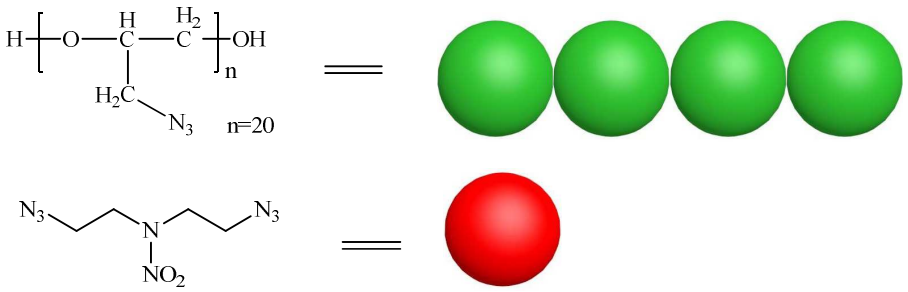

Fig. 3 Coarse-grained models for GAP (up) and DIANP (down)

For each GAP/DIANP blend, a mesoscopic simulation was carried out in a cubic box of 20×20×20. A total of 10^5 time steps with the step size of 0.05 were performed for equilibration. ρ=3 and $\kappa_B T$=1 was chosen to allows a reasonable and efficient relaxation for each blend system, where T and κ_B are temperature and Boltzmann constant, respectively. Radius of interaction, particle mass, dissipation parameter and spring constant all maintain the default values of the program. The repulsion parameter (α_{ij}) between DPD particles was

calculated through the following equations.

$$\alpha_{ij}=\alpha_{ii}+3.50\chi_{ij} \quad (6)$$

$$\alpha_{ii}=75\kappa_B T/\rho \quad (7)$$

Groot and Warren [25] suggested that ρ=3 and hence $\alpha_{ii}=25\kappa_B T$ are reasonable parameters for liquids. Moreover, the binary mixtures studied by Groot and Warren are similar to our systems, i.e., the blends of monomers and polymers. Using ρ=3 in DPD simulations is suitable for GAP/DIANP blends. The bead-bead interactions in these mesoscale models were studied using the Florye-Huggins theory [26-27]. The Flory-Huggins interaction parameter (χ_{ij}) was calculated using the Blends module based on Eq.(8) from the end repeating unit. Parameters in calculations were: 10,000,000 for energy examples, 0.2 kcal.mol^{-1} for energy bin width, 100,000 for cluster examples, and 20 for interactions per cluster. Optimized repeat unit of GAP as the base (b) and DIANP as the screen (s) adopt the "head and tail atoms non-contact" style to reach the purpose of using repeat units instead of polymer.

$$\chi_{ij}=\frac{E_{mix}}{RT} \quad (8)$$

where E_{mix} is the mixing energy, i.e., the difference in free energy between the mixed and the pure states due to interactions. In the traditional Flory-Huggins model, each component occupies a lattice site. For a lattice, the mixing energy is obtained as follows:

$$E_{mix}=\frac{Z_{bs}[E_{bs}(T)]+Z_{sb}[E_{sb}(T)]-Z_{bb}[E_{bb}(T)]-Z_{ss}[E_{ss}(T)]}{2} \quad (9)$$

where Z_{ij} is the coordination number of the lattice, i.e., the number of molecules of component j that can be packed around a single molecule of component i within the excluded-volume constraints. E_{ij} is the binding energy between a unit of component i and a unit of component j. For molecules, the binding energies are averages over an ensemble of molecular configurations. This methodology has been successfully employed in calculating the properties of macromolecules [28-29].

3. Results and discussion

3.1 Criteria of system equilibrium for MD simulation

There are two criteria to judge the equilibrium of MD simulation: one is the

equilibrium of temperature (i.e., the fluctuation of temperature is within ±15K) and another is the equilibrium of energy (i.e., the energy is invariable or has small fluctuation around the average energy value). According to the criteria, all simulated systems have basically reached balance. Fig. 4 shows the fluctuation curves of temperature and energy of GAP3 as an example.

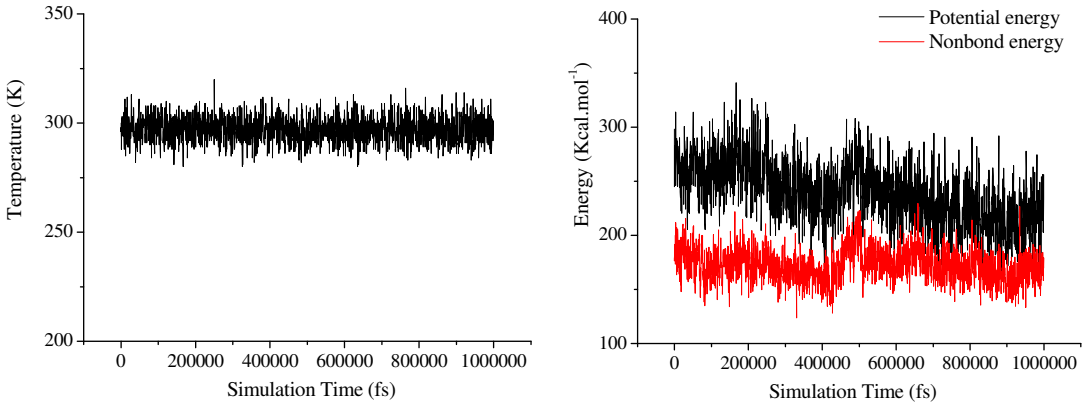

Fig. 4 Fluctuation curves of temperature (left) and energy (right) in the equilibrium run for GAP3 at 298 K

The simulated and experimental densities are reported in Table 3. Clearly, they have a good consistence, which signifies the effective optimization of intermolecular interactions achieved and the packing structure is in reality.

Table 3 Simulated and experimental densities ($g.cm^{-3}$) at 298 K

Species	Experimental density	Simulated density
GAP1	1.30[30]	1.30±0.01
GAP2		1.30±0.01
GAP3		1.30±0.01
GAP4		1.30±0.01
GAP5		1.30±0.00
DIANP	1.33[10]	1.33±0.01

3.2 Solubility parameter (δ)

The solubility parameter is an important physical quantity to measure the compatibility of materials. It was selected as a function to examine appropriate chain lengths of GAP in this work. The simulated δs obtained from the MD simulation calculations are summarized in

Table 4. It is well established, for GAP, that the solubility parameter decreases with the increasing n from 5 to 40 and when n reaches 20, the solubility parameter changes little. Compared with the experimental data (18.0~18.8 $MPa^{0.5}$), it was found that when $n \geq 20$, the predicted δs are consistent well with the experimental data and the higher the n is, the better the agreement is, which follows the common sense. Considering the limitation of computer resources, a chain with 20 repeat units (GAP3) is sufficient to represent the GAP chain and it was adopted in the following study.

According to the Hildebrand semi-empirical formula [31] ($\Delta H_m/V\phi_A\phi_B=(\delta_A-\delta_B)^2$, where V is the total volume, ϕ_A and ϕ_B are the volume fractions and δ_A and δ_B are the solubility parameters of A and B, respectively) and the thermodynamic requirement of formation of a compatible system ($\Delta G_m=\Delta H_m-T\Delta S_m<0$ [32], since ΔS_m is usually positive, hence ΔH_m is the determining factor [33]), we know that the closer the δ_A and δ_B are, the smaller the ΔH_m and ΔG_m are. That is to say, the materials with similar solubility parameters are thermodynamically compatible [34]. To discuss the plasticizing effect of DIANP on GAP, it is necessary to know whether they have a good compatibility first, since the plasticizing is the process that polymer and plasticizer dissolve with each other. Therefore, the δ of DIANP was also calculated and listed in Table 4. The good agreement was observed between the experimental and simulated solubility parameters for DIANP, verifying the reliability of the constructed models and employed method. The difference ($\Delta\delta$) between the solubility parameters of GAP3 and DIANP is 4.22 $MPa^{0.5}$. According to the criteria proposed by Greenhalgh et al. [35], i.e., the system is miscible with $\Delta\delta<7.0$ $MPa^{0.5}$, whereas immiscible with $\Delta\delta>10.0$ $MPa^{0.5}$, it is known that GAP and DIANP are miscible with each other.

Table 4 Cohesive energy density (*CED*) and solubility parameter (δ) of GAP and DIANP

	CED/J. m^{-3}	δ/$MPa^{0.5}$
GAP1	4.897×10^8	22.13
GAP2	4.207×10^8	20.51
GAP3	3.293×10^8	18.42 (18.0~18.8 [36])
GAP4	3.316×10^8	18.21
GAP5	3.283×10^8	18.12
DIANP	5.126×10^8	22.64 (22.29 [9])

3.3 Mechanical properties

Table 5 summarizes the static mechanical properties, including tensile (Young's) modulus (E), bulk modulus (K), shear modulus (G), ratio of bulk modulus and shear modulus (K/G), Poisson's ratio (γ), and Cauchy pressure (C_{12}–C_{44}) of GAP3/DIANP blends (I~III) and pure GAP3. Clearly, γ, K/G, and C_{12}-C_{44} of I, II, and III are comparable to or larger than those of pure GAP; Blend I (with the mass ratio of GAP to DIANP 78.4/21.6) has the largest E and the smallest γ, K/G, and C_{12}-C_{44}; Blend II (with the mass ratio of 57.7/42.3) possesses the second largest E, while the largest γ, K/G, and C_{12}-C_{44}.

Elastic modulus, a measurement of rigidity, is the ratio of stress to strain. The larger the E a material has, the stronger the rigidity is [37]. C_{12}–C_{44} [19] is a criterion to evaluate the ductility and brittleness of a material. The positive value of C_{12}–C_{44} stands for a ductile material and the negative for a brittle material, and the more positive the value is, the more ductile the material is. Poisson's ratio (γ) is associated with the plasticity of a material, and the bigger Poisson's ratio suggests a better plastic property. K/G can be used to evaluate the tenacity of a material. Usually, the greater the value of K/G is, the better tenacity the material possesses [38]. According to these criteria, it can be known that I, II, and III all have better tenacity and ductility than GAP3, indicating that DIANP can enhance the plastic property of GAP. Comparing three blends, II has the best plastic property and I possesses the lowest tenacity and ductility and the highest rigidity. The equilibrium unit cell of II and its initial configuration are shown in Fig. 5.

Table 5 Mechanical properties of GAP3/DIANP blends and pure GAP obtained from MD simulations.

	E/GPa	K/GPa	G/GPa	γ/GPa	K/G	C_{12}-C_{44}/GPa
I	4.00	3.38	1.54	0.30	2.19	0.80
II	2.83	2.87	1.05	0.34	2.73	0.98
III	2.80	2.68	1.06	0.33	2.54	0.84
GAP	4.49	3.75	1.73	0.30	2.17	0.67

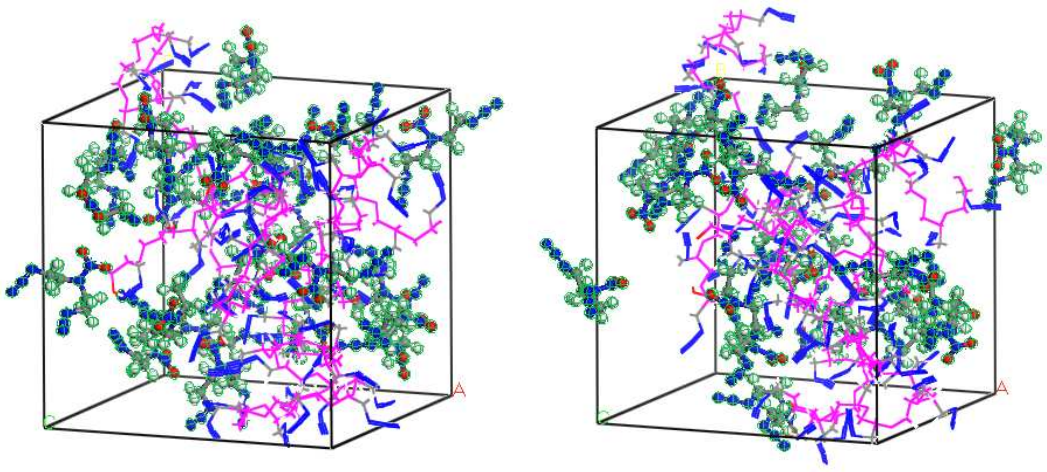

Fig. 5 Equilibrium structure (right) of II relative to its initial configuration (left) at 298 K (Ball and stick for DIANP and line for GAP3)

3.4 Flory–Huggins parameters

To investigate how the number of repeat units in one GAP bead affects the Flory-Huggins interaction parameter, we chose different GAP repeat units as the base and one DIANP molecule as the screen to calculate E_{mix} and χ_{ij} (Table 6). With the increasing number of the repeat units of GAP, χ_{ij} shows the tendency of increase (Fig. 6a), which means that the calculated χ_{ij} relies heavily on the number of repeat units of base. Since C_n of GAP is 5.299, thus N_{DPD} of a GAP chain is about 4 in the coarse-grained model (Fig. 3), that is to say, five repeat units as a bead to calculate χ_{ij} (6.50) is suitable for this research. Fig. 6b plots the binding energy distributions of the blend with 5 GAP repeat units as base and 1 DIANP as screen. It can be seen that GAP and DIANP are miscible with each other since the blend binding energy distributions of E_{bs}, E_{bb} and E_{ss} are similar with each other, as was found from the analysis of the solubility parameter.

Table 6 Flory-Huggins interaction parameters (298K) obtained with different number of GAP repeat units as base

Number of GAP repeat units (base)	Number of DIANP molecule (screen)	E_{mix}/kcal.mol^{-1}	χ_{ij}
1	1	-1.08	-1.83
5	1	3.85	6.50
10	1	14.55	24.56
15	1	14.17	23.93
20	1	27.47	46.40

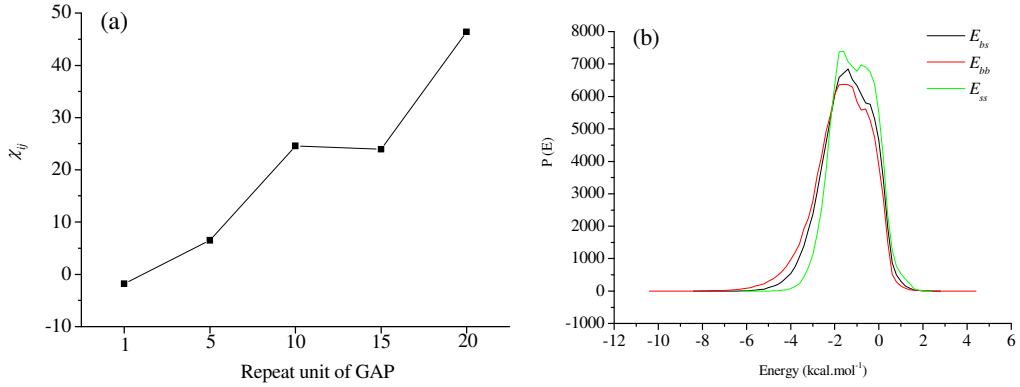

Fig. 6 Flory–Huggins parameters (χ_{ij}) obtained at 298 K (a) and blend binding energy distributions with 5 GAP repeat units as base and 1 DIANP as screen (b)

3.5 Criteria of system equilibrium for DPD simulation

To further investigate the compatibility of GAP and DIANP, DPD simulations were carried out for three GAP/DIANP blending systems (I, II, and III). The variation trends of the diffusivity with simulation times are shown in Fig. 7. Clearly, I, II, and III all have reached equilibrium when the simulation time is up to 3000. When the simulation continues, diffusion coefficients do not change any more. In addition, the diffusivity of GAP is better than DIANP, and the large difference of diffusivity between GAP and DIANP may attribute to the intensive mixing of the bending systems.

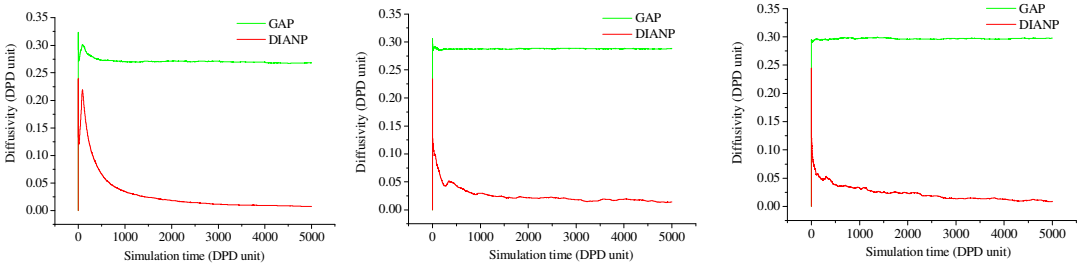

Fig. 7 Change of diffusivity during simulations for I, II, and III

3.6 Morphologies and radial distribution functions

Fig. 8 illustrates the morphologies of three blends after 10^5 time steps of DPD simulation and in the figure no phase separation was observed. For quantitatively comparing

the system of GAP and DIANP, Fig. 9 shows the intermolecular pair correlation functions of GAP-GAP, DIANP-DIANP, and GAP-DIANP in blends II. Here, the pair correlation functions were based on the center-of-mass for each molecule. The pair correlation function gives a measure of the probability to find another particle at a distance r from a specific particle. It can reflect the characteristics of the microstructure and reveal the essence of the interaction between non-bonding atoms. Obviously, intermolecular pair correlation functions of the two compounds are similar with each other (black and red line in Fig.9). Following the principle that the similar substance is more likely to be dissolved by each other, the similar pair correlation functions verified that GAP and DIANP have good compatibility. In addition, for the binary blending system (A/B), if the $g(r)$ of A-B ($g_{A\text{-}B}$) is higher than those of A-A and B-B ($g_{A\text{-}A}$ and $g_{B\text{-}B}$), the system will possess a good compatibility, otherwise, phase separation will happen [39]. Clearly, the green line is higher than red and black lines when the distances are lower than 7.0 Å (the distances of 2.6–3.1, 3.1–5.0 and above 5.0 Å belong to hydrogen bonding, strong vdW, and weak vdW forces, respectively), suggesting the interactions between GAP and DIANP is higher than their respective intermolecular interactions and revealing the good compatibility between GAP and DIANP once again. Good agreements were achieved with the analyses of the solubility parameters and Flory–Huggins parameters.

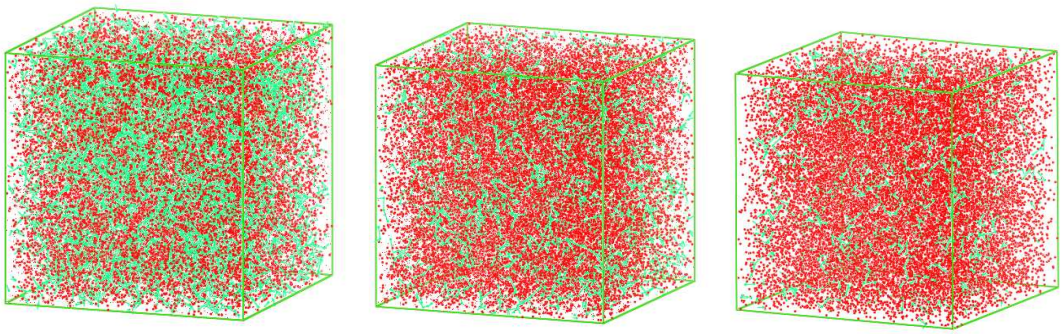

I II III

Fig. 8 Morphologies of three blends after 10^5 time steps

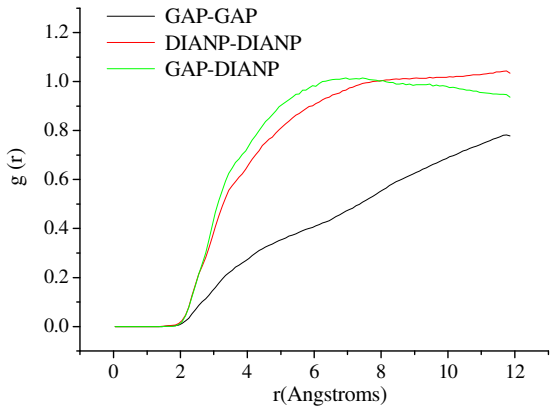

Fig. 9 Intermolecular pair correlation functions in blend II

4. Conclusions

In this study, a series of polymer blends of GAP and DIANP with different mass ratios (GAP/DIANP=78.4/21.6 (I), 57.7/42.3 (II), and 37.7/62.3 (III)) were investigated by molecular dynamics (MD) and dissipative particle dynamics (DPD) simulations. Solubility parameters, Flory–Huggins parameters and morphologies of the binary blending systems give a consistent conclusion, that is, DIANP has a good miscibility with GAP. Mechanical properties of three GAP/DIANP blends (I, II, and III) and pure GAP were investigated and compared. The results show that DIANP can enhance the plastic property of GAP and the blend II has the best tenacity and ductility. It is the first time that the miscibility and the mechanical properties of the azido plasticizer DIANP and the azido binder GAP were investigated theoretically. It will be helpful for better understanding the plasticizer DIANP and can give useful guidance on the design of GAP/DIANP composite propellants.

Acknowledgments

We gratefully thank the National Natural Science Foundation of China (NO. 21403110), the Research Fund for Natural Science Foundation of Jiangsu Province (NO. BK20130755), and the "Excellent Plan and Zijin Star" Research Foundation of NUST for their support to this work.

Reference

1. Y. Zhou, X. P. Long and Q. X. Zeng, *Journal of Applied Polymer Science*, 2012, **125**, 1530-1537.
2. S. Mathew, S. e. K. Manu and T. e. L. Varghese, *Propellants, Explosives, Pyrotechnics*, 2008, **33**, 146-152.
3. Y. Zhou, X. P. Long and Q. X. Zeng, *Journal of Applied Polymer Science*, 2013, **129**, 480-486.
4. Y. M. Mohan, M. P. Raju and K. M. Raju, *International Journal of Polymeric Materials*, 2005, **54**, 651-666.
5. *US 4141910 Pat.*, 1979.
6. R. D. Groot, T. J. Madden and D. J. Tildesley, *The Journal of Chemical Physics*, 1999, **110**, 9739-9749.
7. C. Soto-Figueroa, L. Vicente, J.-M. Martínez-Magadán and M.-d.-R. Rodríguez-Hidalgo, *Polymer*, 2007, **48**, 3902-3911.
8. H.-J. Qian, Z.-Y. Lu, L.-J. Chen, Z.-S. Li and C.-C. Sun, *Macromolecules*, 2005, **38**, 1395-1401.
9. Y. P. Ji, F. L. Gao, R. Han, B. Chen, Y. L. Wang, W. X. Liu, Y. J. Liu and Y. L. Yao, *Chinese Journal of Energetic Materials*, 2013, **21**, 612-615.
10. J. L. Wang, Y. P. Ji, F. L. Gao, W. Guo and S. T. Ren, *Chinese Journal of Energetic Materials*, 2011, **19**, 693-696.
11. J. Yang, F. Wang, J. Zhang, G. Wang and X. Gong, *Journal of Molecular Modeling*, 2013, 5367-5376.
12. Z. Luo and J. Jiang, *Polymer*, 2010, **51**, 291-299.
13. *Accelry Inc: San Diego, CA*.
14. Q. Wang, N. S. Suraweera, D. J. Keffer, S. Deng and J. Mays, *Macromolecules*, 2012, **45**, 6669-6685.
15. Q. Wang, D. J. Keffer, S. Deng and J. Mays, *Polymer*, 2012, **53**, 1517-1528.
16. J. Gupta, C. Nunes, S. Vyas and S. Jonnalagadda, *The Journal of Physical Chemistry B*, 2011, **115**, 2014-2023.
17. L. Huynh, J. Grant, J.-C. Leroux, P. Delmas and C. Allen, *Pharmaceutical research*, 2008, **25**, 147-157.
18. K. Pajula, M. Taskinen, V.-P. Lehto, J. Ketolainen and O. Korhonen, *Molecular pharmaceutics*, 2010, **7**, 795-804.
19. J. H. Weiner, *Statistical Mechanics of Elasticity*, New York, 1983.
20. H. Sun, *The Journal of Physical Chemistry B*, 1998, **102**, 7338-7364.
21. H. C. Andersen, *The Journal of chemical physics*, 1980, **72**, 2384-2393.
22. M. P. Allen and D. J. Tildesley, *Computer Simulation of Liquids*, Oxford University Press, New York, 1989.
23. M. Doi and S. F. Edwards, *The theory of polymer dynamics*, Oxford: Oxford University Press, 1988.
24. J. Bicerano, *Prediction of Polymer Properties*, CRC Press, Prediction of polymer properties, 2002.
25. R. D. Groot and P. B. Warren, *Journal of Chemical Physics*, 1997, **107**, 4423.
26. P. J. Flory, *The Journal of chemical physics*, 1941, **9**, 660-661.
27. M. L. Huggins, *Journal of Chemical Physics*, 1941, **9**, 440-449.
28. C. Soto-Figueroa, L. Vicente, J.-M. Martínez-Magadán and M.-d.-R. Rodríguez-Hidalgo, *The Journal of Physical Chemistry B*, 2007, **111**, 11756-11764.
29. L. Vicente, C. Soto, H. Pacheco-Sánchez, J. Hernández-Trujillo and J. M. Martinez-Magadán, *Fluid phase equilibria*, 2006, **239**, 100-106.
30. K. Selim, S. Özkar and L. Yilmaz, *Journal of Applied Polymer Science*, 2000, **77**, 538-546.

31. J. H. Hildebrand and R. L. Scott, *Solubility of Non-electrolytes*, Reinhold Publishing Corp, New York, 1936.
32. B. Schneier, *Journal of Applied Polymer Science*, 1973, **17**, 3175-3185.
33. A. F. Barton, *CRC Handbook of Solubility Parameters and Other Cohesion Parameters*, CRC press, Boca Raton, 1991.
34. J. N. Lee, C. Park and G. M. Whitesides, *Analytical Chemistry*, 2003, **75**, 6544-6554.
35. D. J. Greenhalgh, A. C. Williams, P. Timmins and P. York, *Journal of Pharmaceutical Sciences*, 1999, **88**, 1182-1190.
36. Z. B. Hu and X. X. Gan, *Chinese Journal of Energetic Materials*, 2004, **12**, 62-62.
37. H. C. Andersen, *The Journal of Chemical Physics*, 2008, **72**, 2384-2393.
38. S. Pugh, *Philosophical Magazine*, 1954, **45**, 823-843.
39. T. C. Clancy, M. Pütz, J. D. Weinhold, J. G. Curro and W. L. Mattice, *Macromolecules*, 2000, **33**, 9452-9463.